



Hydrogen Sulfide sensing characteristics of Spinel-type Nanocrystalline $\text{Zn}_{0.7}\text{Mg}_{0.3}\text{Co}_2\text{O}_4$

T.R. Tatte^{1*} and V.D. Kapse²

¹Department of Physics, Government Vidarbha Institute of Science & Humanities, Amravati 444604, Maharashtra, India

²Department of Physics, Arts, Science and Commerce College, Chikhaldara 444807, Maharashtra State, India
truptitatte21@gmail.com

Available online at: www.isca.in, www.isca.me

Received 2nd October 2016, revised 4th December 2016, accepted 16th December 2016

Abstract

Nanocrystalline $\text{Zn}_{1-x}\text{Mg}_x\text{Co}_2\text{O}_4$ ($x = 0.3$) spinel having cubic structure was synthesized by sol-gel method successfully calcined at 500°C for 2 h. The formation of $\text{Zn}_{1-x}\text{Mg}_x\text{Co}_2\text{O}_4$ confirms by means of an X-ray powder diffraction (XRD) and Fourier Transform-Infra-red spectrum (FT-IR). Scanning electron microscopy (SEM) was examined the surface morphology. To study hydrogen sulfide gas sensing characteristics of $\text{Zn}_{1-x}\text{Mg}_x\text{Co}_2\text{O}_4$ spinel were systematically investigated. $\text{Zn}_{1-x}\text{Mg}_x\text{Co}_2\text{O}_4$ showed excellent gas sensing properties like, high gas response towards 50 ppm hydrogen sulfide gas at 100°C , good selectivity at lower operating temperature 100°C . The response and recovery time for $\text{Zn}_{1-x}\text{Mg}_x\text{Co}_2\text{O}_4$ were found to be 16 s and 52 s respectively. The results proved that nanocrystalline $\text{Zn}_{1-x}\text{Mg}_x\text{Co}_2\text{O}_4$ is a potential candidate for detection of hydrogen sulfide. Moreover, possible hydrogen sulfide sensing mechanism is discussed.

Keywords: $\text{Zn}_{1-x}\text{Mg}_x\text{Co}_2\text{O}_4$, Nanocrystalline, Spinel, XRD, SEM, Gas response.

Introduction

Extensive research is being carried out in the fields of environmental monitoring, air quality detection, food, inflammable-gas inspection, health, energy optimization and security due to their prospective applications in the field of gas sensors^{1,2}. Oxide semiconductor gas sensors are widely investigated due to their high sensitivity, cost effectiveness, and reliability. The sensitivity of the sensor is influenced by many factors, and the sensitivity is enhanced by surface modification, doping with noble metals and composite formation, etc.^{3,4}.

Generally, spinel have a formula MY_2O_4 , in which M and Y is a divalent metal and trivalent respectively. In chemical processes, ZnCo_2O_4 act as effective catalysts such as CO oxidation⁵ reduction of several organic molecules and catalytic combustion of hydrocarbons⁶⁻⁸. In cobalt based ZnCo_2O_4 cubic spinel structure, where, Zn divalent ions occupy the tetrahedral and Co trivalent ions occupy octahedral site⁹.

Nano structured ZnCo_2O_4 is stable and cheaper than noble metals¹⁰. Moreover, it is also active in alkaline solutions. Conventional methods involving high temperature reactions mixing with oxides properly and do not constantly yield single phase materials for the synthesis of cobalt based oxides¹¹. Furthermore, finally the products are inhomogeneous, non-stoichiometric having low specific surfaces and hence, reducing their efficiency in catalysis. Recently, some typical synthesis methods such as co-precipitation, sol-gel route, hydrothermal synthesis, etc. used to prepare spinel-types oxide in the form of nanoparticles. Recently, template assisted method is used to

prepare nanotubes MCo_2O_4 ($\text{M} = \text{Ni}, \text{Cu}, \text{Zn}$) and also, their gas sensing properties to Cl_2 , NO_2 , $\text{C}_2\text{H}_5\text{OH}$, SO_2 investigated¹². Moreover, microemulsion method is used to synthesize nanocrystalline ZnM_2O_4 ($\text{M} = \text{Fe}, \text{Co}, \text{Cr}$) and their NO_2 , Cl_2 , $\text{C}_2\text{H}_5\text{OH}$ and H_2S gas sensing properties is also discussed.

In this work, we devote to investigate nanostructured $\text{Zn}_{0.7}\text{Mg}_{0.3}\text{Co}_2\text{O}_4$ is a good sensing material for hydrogen sulfide with higher gas response as well as good selectivity and its average grain size is ~ 28 nm. The present investigation was illustrated to explain nanocrystalline $\text{Zn}_{0.7}\text{Mg}_{0.3}\text{Co}_2\text{O}_4$ have excellent hydrogen sulfide sensing properties.

Materials and Methods

Preparation of $\text{Zn}_{0.7}\text{Mg}_{0.3}\text{Co}_2\text{O}_4$ powder: Firstly, cobaltous nitrate, magnesium nitrate, and zinc nitrate were dissolving in ethanol. All the chemicals were mixed in a good manner with each other. Then, adding ethanol solution of oxalic acid to above mixture under magnetic stirring at a room temperature and continuous stirring for 3 h and then mixture was evaporated at 80°C for 1 h, forming a sol and after then the sol was heated at 100°C for 1 h until formation of gel. Consequently, oxalate precursor powder was obtained after drying the gel in an electric oven for 1 h. The final prepared powder was sintered at 500°C for 2 h which led to the formation of well-crystalline $\text{Zn}_{0.7}\text{Mg}_{0.3}\text{Co}_2\text{O}_4$ powder.

The structural and morphological properties of the prepared sample was studied by X-ray diffractometer using a Goniometer MiniFlex 300/600 equipped with Cu $\text{K}\alpha$ radiation ($\lambda = 1.5406$

A^o) and accelerating voltage 40 kV and current 15 mA and the resulting data were analyzed using JCPDS standards. The structural coordination in the powder sample were recorded by FTIR system and obtained spectrum in the range 400–4000 cm⁻¹ were analysis using 3000 Hyperion Microscope with Vertex 80 (Bruker, Germany).

Fabrication of sensor and measurement of gas-sensing properties: Nanostructured Zn_{1-x}Mg_xCo₂O₄ powder sample was mixed in butyl cellulose, butyl carbitol acetate and turpineol solvents with ethyl cellulose solution using as a temporary binder. The obtained paste was printing onto a glass substrate by screen printing technology and fired the prepared thick films at 500°C for 1h. The particle morphology of prepared thick film was measured by SEM using JSM-7600F microscope with an accelerating voltage of 0.1 to 30 kV.

Nanostructured Zn_{1-x}Mg_xCo₂O₄ oxide thick films so prepared and for the formation of the sensing element, the ohmic contacts were done by depositing the film with silver paste by using thermal evaporation technique. To study the behaviour of test gas in air, the sensing element was placed in contact with the sensor in a static gas chamber and put sensing element on a heater directly by varying the temperature from 27 to 400°C. The chromel–alumel thermocouple is used for monitoring the operating temperature of the sensing element. For gas sensing characteristics measurement, the known volume of the test gas was injected with a micro-syringe in desired concentration into the gas chamber, maintaining atmospheric pressure. The electrical resistance of sensor in presence and absence of test

gas was calculated. After approximately 90 s, open the chamber to the atmosphere and recovery of sensor was studied and the gas response (S) can be calculated as:

$$S = \frac{R_{air}}{R_{gas}} \quad (1)$$

Where: R_{air} and R_g are the electrical resistance in air and in the presence of a test gas respectively.

Results and Discussion

XRD analysis: The XRD pattern of Zn_{0.7}Mg_{0.3}Co₂O₄ oxide calcined at 500°C for 2 h is shown in Figure-1. XRD peaks appeared at (111), (220), (311), (222), (400), (331), (422), (511), (440), (531), (533), (622), (444) and 2θ values 19.9°, 36.65°, 59.19° and 65.8° which exhibits the formation of Zn_{0.7}Mg_{0.3}Co₂O₄ spinel structure with Fd3m space group. By using the Debye– Scherrer equation, the crystallite size was calculated:

$$D = \frac{k\lambda}{B\cos\theta} \quad (2)$$

Where: D is the average crystallite size, k is 0.9, λ is the wavelength of X-ray source, B is the peak full width at half maximum (FWHM) intensity (in radians) and θ is the angle of diffraction. The crystallite size of Zn_{0.7}Mg_{0.3}Co₂O₄ oxide is found to be 18 nm.

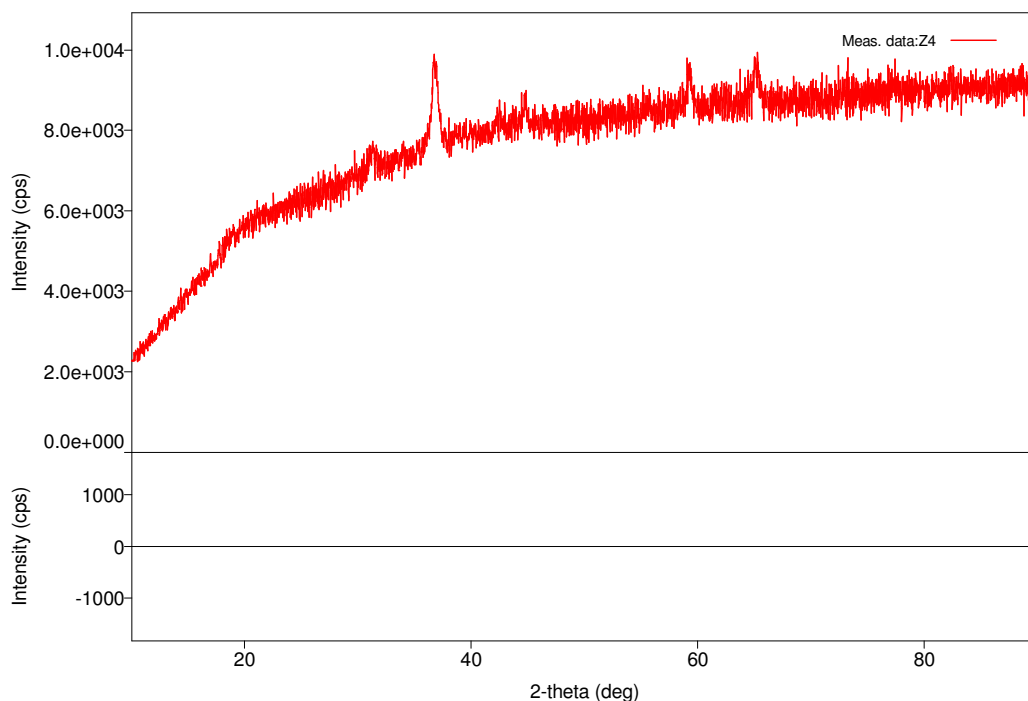


Figure-1
XRD pattern of nanocrystalline Zn_{0.7}Mg_{0.3}Co₂O₄ annealed at 500°C

FTIR analysis: FTIR spectrum of nanocrystalline $\text{Zn}_{0.7}\text{Mg}_{0.3}\text{Co}_2\text{O}_4$ is presented in Figure-2. Generally, vibrations of metal ions in the crystal lattice are in the range of $400\text{--}4000\text{ cm}^{-1}$ in FTIR analysis. It can be observed that two strong absorption bands are presented at 659 and 565 cm^{-1} and these bands coincides with spinel ZnCo_2O_4 . The peak at 667 cm^{-1} observed corresponds to the vibration of metal ions for the tetrahedral site and the band at 572 cm^{-1} assigned to the octahedral metal ions.

SEM analysis: SEM image of nanocrystalline $\text{Zn}_{0.7}\text{Mg}_{0.3}\text{Co}_2\text{O}_4$ oxide is as shown in Figure-3. For finding morphology of the powder, SEM technique was used. From figure, it shows the formation of the agglomerated particle having grain size is $\sim 28\text{ nm}$. SEM image exhibit that the nanocrystalline $\text{Zn}_{0.7}\text{Mg}_{0.3}\text{Co}_2\text{O}_4$ thick film show structure having large grains size with soft agglomerations has a regular morphology (polygons).

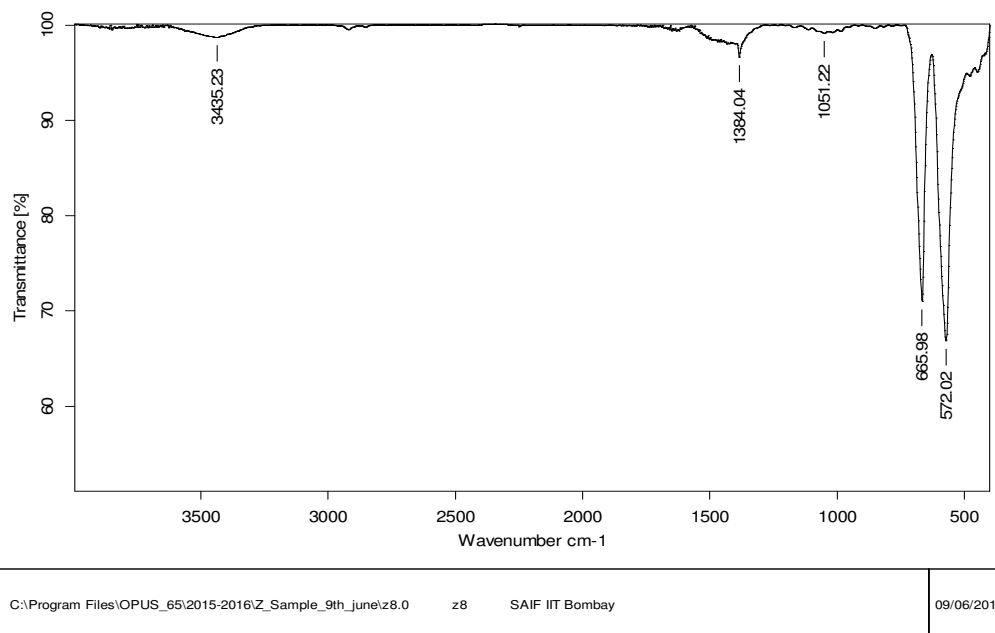
Energy dispersion X-ray analysis: Energy dispersion X-ray analysis (EDX) was investigated the presence of elements in synthesized $\text{Zn}_{0.7}\text{Mg}_{0.3}\text{Co}_2\text{O}_4$ thick film. EDX spectrum of the nanocrystalline $\text{Zn}_{0.7}\text{Mg}_{0.3}\text{Co}_2\text{O}_4$ is as shown in Figure-4. The EDX analysis exhibit the presence of Mg, Zn, Co, and O and in EDX spectrum almost the same ratio of Mg/Zn/Co for the nanocrystalline $\text{Zn}_{0.7}\text{Mg}_{0.3}\text{Co}_2\text{O}_4$ are observed as they were adding during synthesis process. Hence, confirms the purity of nanocrystalline $\text{Zn}_{0.7}\text{Mg}_{0.3}\text{Co}_2\text{O}_4$.

Gas sensing properties: Nanocrystalline $\text{Zn}_{0.7}\text{Mg}_{0.3}\text{Co}_2\text{O}_4$ thick film was prepared for investigation of gas-sensing characteristics. The prepared thick films were then subjected for

studying their sensitivity and selectivity at the optimal operating temperatures towards various gases.

The gas response towards a specificity of gas needs to be manifestly higher than to the other test gases. The selective behavior of nanocrystalline $\text{Zn}_{0.7}\text{Mg}_{0.3}\text{Co}_2\text{O}_4$, gas response (S) towards various gases such as (LPG), (NH_3), (CO_2), (H_2S), (Cl_2), (H_2) and ($\text{C}_2\text{H}_5\text{OH}$) is shown in Figure-5. Nanocrystalline $\text{Zn}_{0.7}\text{Mg}_{0.3}\text{Co}_2\text{O}_4$ exhibits the higher response towards H_2S to 50 ppm concentration as compared to the other test gases. All the gases such as hydrogen, LPG, ammonia, CO_2 , Cl_2 and ethanol vapors appears lower gas response and shows gas response (S) below 2 as compared to H_2S . Whereas, H_2S have higher gas response 18.31 to the other test gases. Gas response (S) of nanocrystalline $\text{Zn}_{0.7}\text{Mg}_{0.3}\text{Co}_2\text{O}_4$ towards H_2S to 50 ppm is as shown in Figure-6. It can be seen that nanocrystalline $\text{Zn}_{0.7}\text{Mg}_{0.3}\text{Co}_2\text{O}_4$ exhibited the higher response to 50 ppm towards H_2S at 100°C .

In general, gas sensing mechanism is discussed in the basis of conductance by adsorption of oxygen on the surface with the test gases. The oxygen on the surface adsorbs by extracting an electron from conduction band which are mainly due to the responsible for detecting test gases. Due to adsorption of oxygen, the deficiency of electrons occurred and the conductivity of thick film decreased. Moreover, optimal operating temperature increases as well as causes oxidation of large extent of hydrogen sulfide molecules and consequentially increases very large number of electron conductivity. This is the main reason behind the gas response increasing with increasing operating temperature.



Page 1/1
Figure-2

FTIR spectra of nanocrystalline $\text{Zn}_{0.7}\text{Mg}_{0.3}\text{Co}_2\text{O}_4$ powder

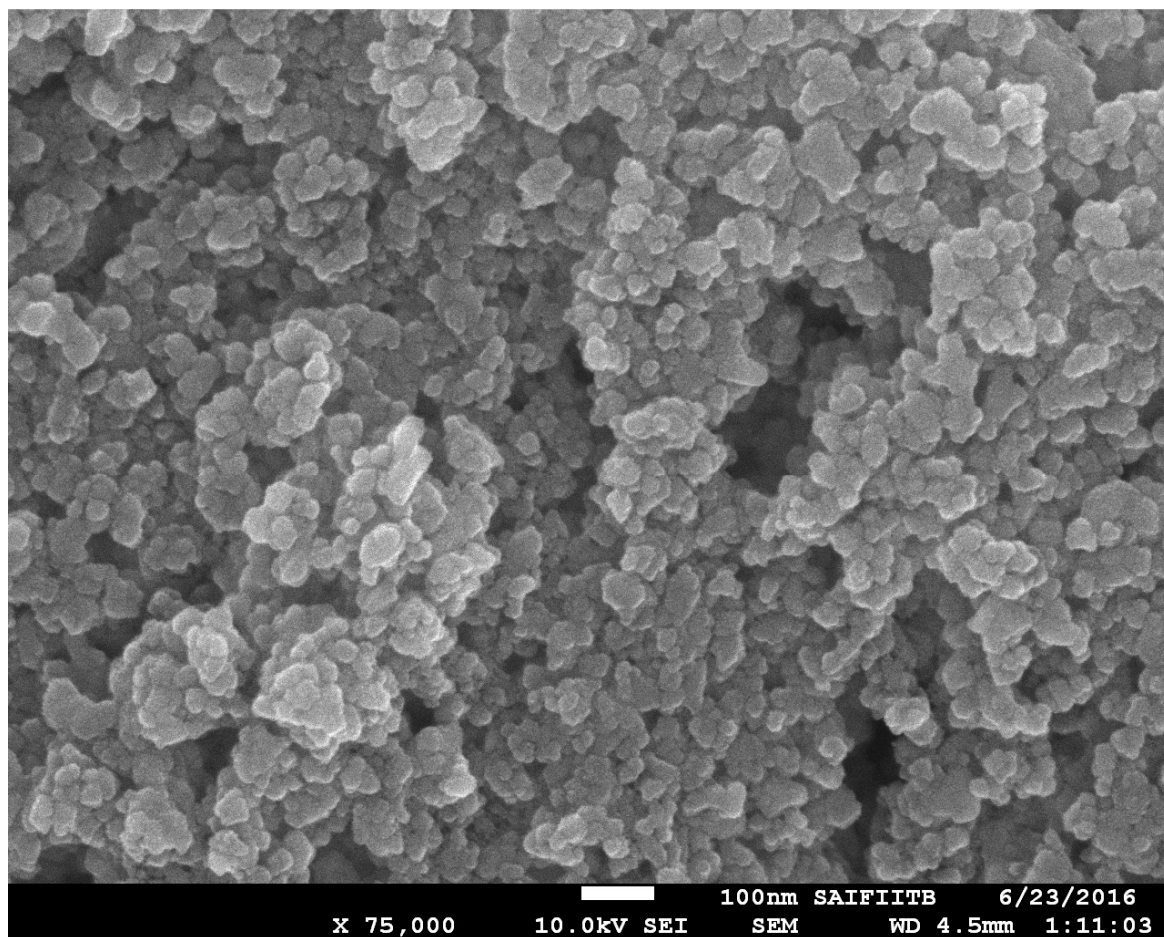


Figure-3
SEM image of nanocrystalline $\text{Zn}_{0.7}\text{Mg}_{0.3}\text{Co}_2\text{O}_4$

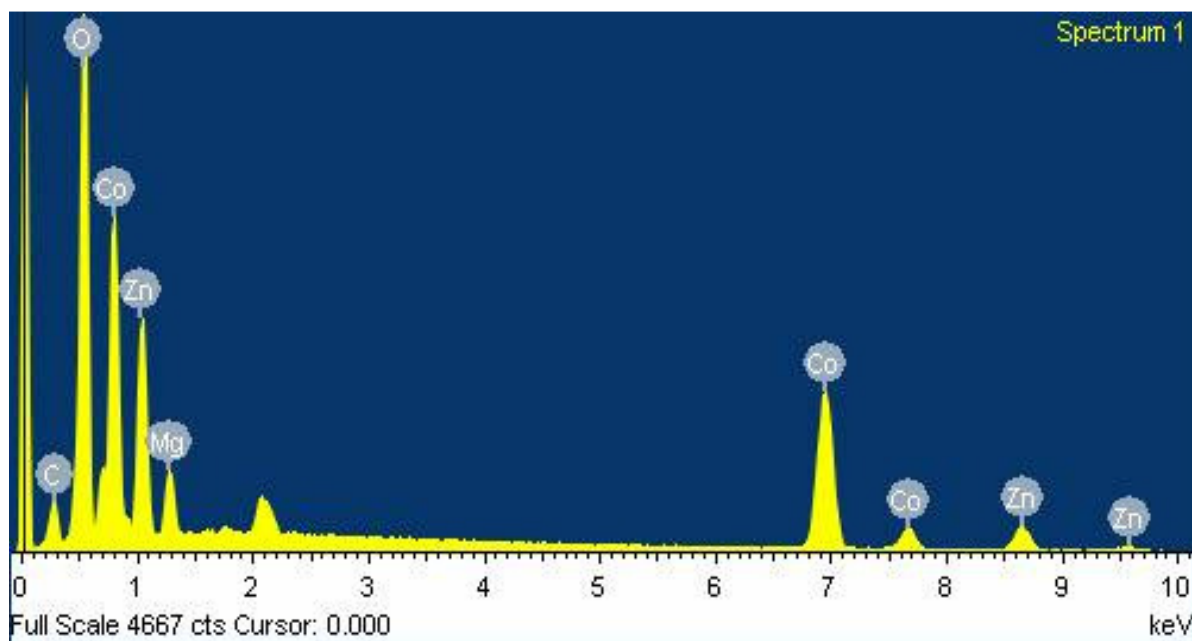


Figure-4
EDX spectrum for nanocrystalline $\text{Zn}_{0.7}\text{Mg}_{0.3}\text{Co}_2\text{O}_4$

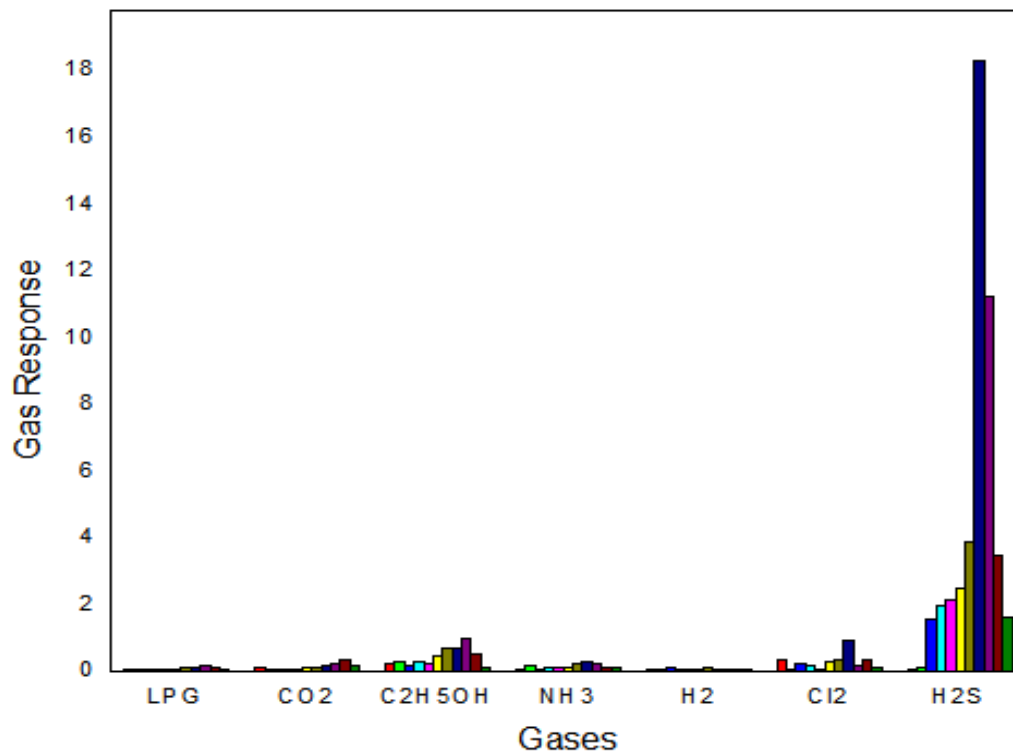


Figure-5

Response of nanocrystalline spinel $\text{Zn}_{0.7}\text{Mg}_{0.3}\text{Co}_2\text{O}_4$ towards 50 ppm of various gases at 100°C

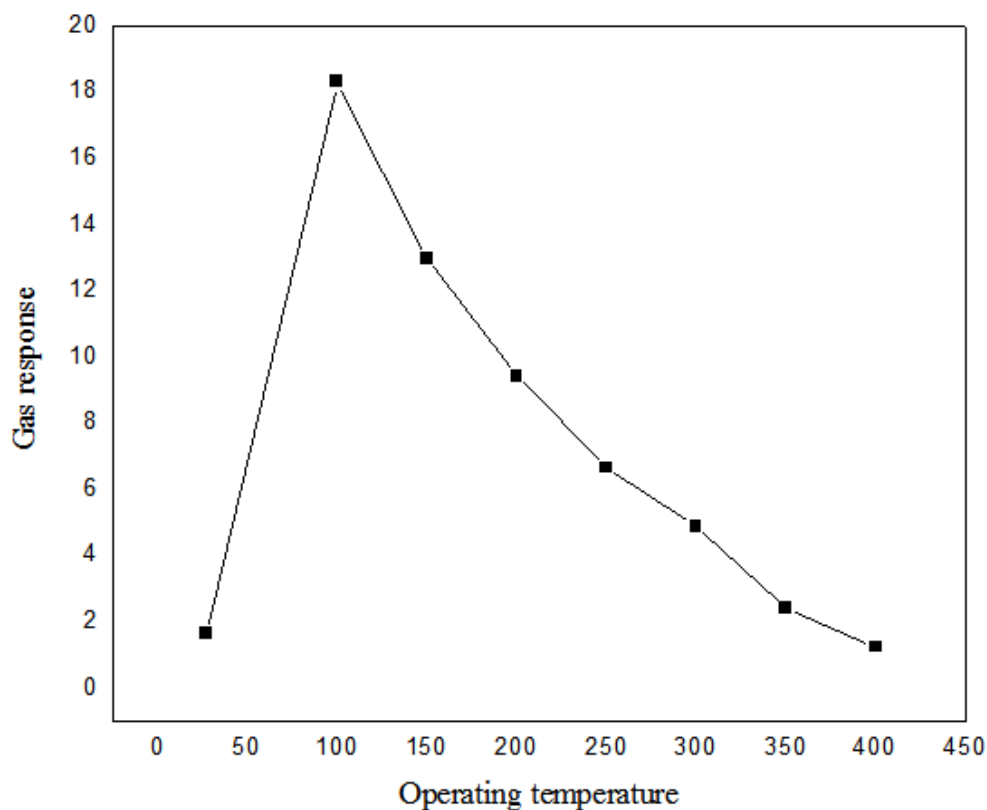


Figure-6

Response of nanocrystalline spinel $\text{Zn}_{0.7}\text{Mg}_{0.3}\text{Co}_2\text{O}_4$ towards hydrogen sulfide; at the operating temperatures

The gas response of nanocrystalline $\text{Zn}_{0.7}\text{Mg}_{0.3}\text{Co}_2\text{O}_4$ based thick film with respect to the hydrogen sulfide concentration to 50 ppm at the optimal operating temperature of 100°C is as shown in Figure-7, which indicates that $\text{Zn}_{0.7}\text{Mg}_{0.3}\text{Co}_2\text{O}_4$ responds as low as 5 ppm of hydrogen sulfide and the response increases linearly with its concentration. The response and recovery time of the gas sensor are another elementary parameter. The response and recovery times are defined as the time taken for the sensor to attain 90% of the maximum increases in conductance on exposure of the target gas is known as response time and the time taken by the sensor to get back 90% of the maximum conductance when the flow of gas is switched off. Figure-8 depicts the response and recovery curve of $\text{Zn}_{0.7}\text{Mg}_{0.3}\text{Co}_2\text{O}_4$ based sensor to 50 ppm hydrogen sulfide at 100°C . It is observed that nanocrystalline $\text{Zn}_{0.7}\text{Mg}_{0.3}\text{Co}_2\text{O}_4$ based sensor responds quickly after introduction of 50 ppm hydrogen sulfide gas and recovers immediately after exposing to air. The nanocrystalline $\text{Zn}_{0.7}\text{Mg}_{0.3}\text{Co}_2\text{O}_4$ have quick response time 16 s and fast recovery time 52 s. Therefore, nanocrystalline $\text{Zn}_{0.7}\text{Mg}_{0.3}\text{Co}_2\text{O}_4$ based sensor exhibits the good response and recovery time to hydrogen sulfide.

The reproducible nature of nanocrystalline $\text{Zn}_{0.7}\text{Mg}_{0.3}\text{Co}_2\text{O}_4$ based sensor to 50 ppm hydrogen sulfide was measured for a month in the interval of 10 days and result as shown in Figure-9. From figure it was found that nanocrystalline $\text{Zn}_{0.7}\text{Mg}_{0.3}\text{Co}_2\text{O}_4$ based sensor possesses a very good stability and durability. On conclusion, the nanocrystalline $\text{Zn}_{0.7}\text{Mg}_{0.3}\text{Co}_2\text{O}_4$ based thick film sensor has excellent gas response to hydrogen sulfide gas at 100°C , good selectivity, quick response as well as fast recovery and excellent repeatability.

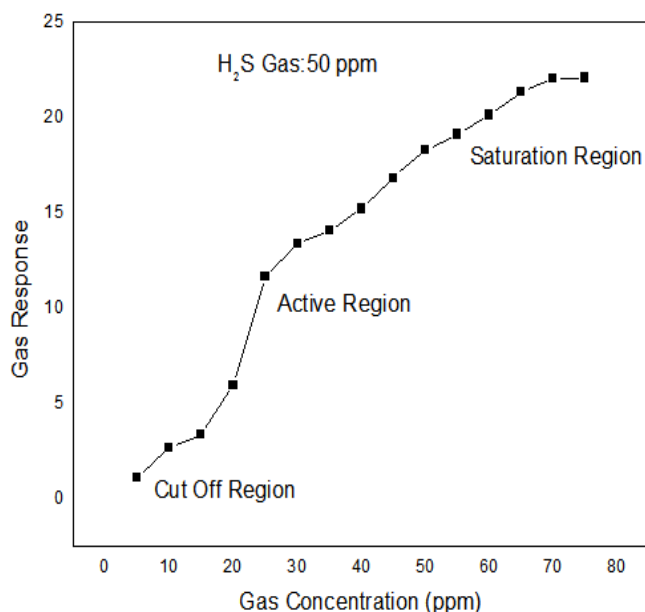


Figure-7

Response towards various gas concentrations (ppm) of hydrogen sulfide

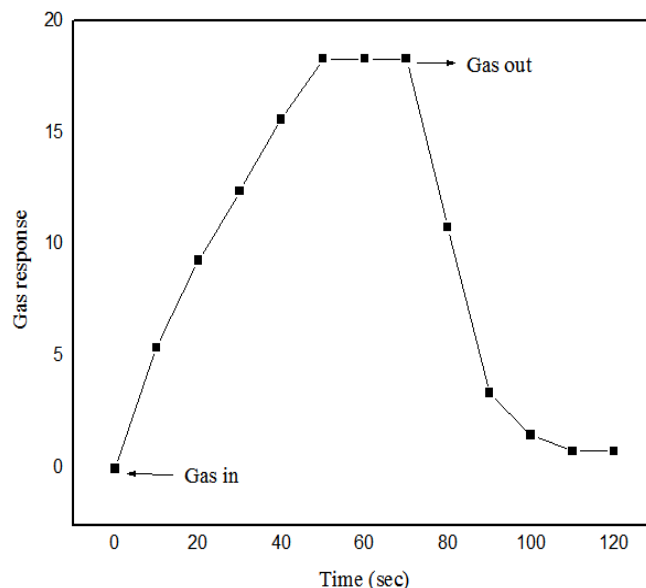


Figure-8

Response and recovery characteristics of sensor to 50 ppm hydrogen sulfide

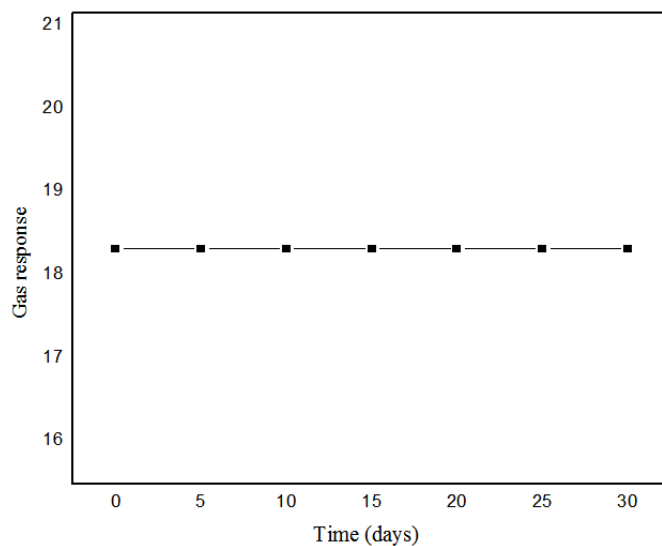


Figure-9

Long-time stability curve of $\text{Zn}_{0.7}\text{Mg}_{0.3}\text{Co}_2\text{O}_4$ sensor

Conclusion

Nanocrystalline spinel-type $\text{Zn}_{0.7}\text{Mg}_{0.3}\text{Co}_2\text{O}_4$ have good gas-sensing properties could be obtained. The spinel-type $\text{Zn}_{0.7}\text{Mg}_{0.3}\text{Co}_2\text{O}_4$ oxide exhibited excellent gas response to hydrogen sulfide at 100°C due to its smaller crystallite size. $\text{Zn}_{0.7}\text{Mg}_{0.3}\text{Co}_2\text{O}_4$ sensor annealed at 500°C showed excellent sensitivity, selectivity, stability, quick response and fast recovery to hydrogen sulfide gas sensing properties. Hence, in short this means that $\text{Zn}_{0.7}\text{Mg}_{0.3}\text{Co}_2\text{O}_4$ sensor can be a good candidate for detecting hydrogen sulfide gas because of the good characteristics mentioned.

Acknowledgement

I gratefully acknowledge Sophisticated Analytical Instrument Facility (SAIF), Indian Institute of Technology (I.I.T.), Bombay for carrying out FT-IR, SEM-EDAX and TEM-ED characterizations and Department of Physics, Vidyabharati Mahavidhyalaya, Amravati for providing the XRD facility.

References

1. Xu S. and Shi Y. (2009). Low temperature high sensor response nano gas sensor using ITO nanofibers. *Sens. Actuators B*, 143, 71–75.
2. Yun S., Lee J., Yang J. and Lim S. (2010). Hydrothermal synthesis of Al-doped ZnO nanorods arrays on Si substrate. *Physica B*, 405, 413–419.
3. Wang C., Yin L., Zhang L., Xiang D. and Gao R. (2010). Metal Oxide Gas Sensors: Sensitivity and Influencing Factors. *Sensors*, 10, 2088-2106.
4. Basu S. and Basu P.K. (2009). Nanocrystalline Metal Oxides for Methane Sensors: Role of Noble Metals. *J. Sensors*, 20, 861968.
5. Ghose J. and Murthy K.S.R.C. (1996). Activity of Cu^{2+} Ions on the Tetrahedral and Octahedral Sites of Spinel Oxide Catalysts for CO Oxidation. *J. Catal.*, 162, 359-360.
6. Yang B.L., Cheng D.S. and Lee S.B. (1991). Effect of steam on the oxidative dehydrogenation of butene over magnesium ferrites with and without chromium substitution. *Appl. Catal.*, 70, 161-173.
7. Jacobs J.P., Maltha A., Reintjes J.G.H., Drimal J., Ponc V. and Brongersma H.H. (1994). The Surface of Catalytically Active Spinel. *J. Catal.*, 147, 294-300.
8. Sloczynski J., Zi'olowski J., Grzybowska B., Grabowski R., Jachewicz D., Wcislo K. and Gengembre L. (1999). Oxidative Dehydrogenation of Propane on $\text{Ni}_x\text{Mg}_{1-x}\text{Al}_2\text{O}_4$ and NiCr_2O_4 Spinel. *J. Catal.*, 187, 410-418.
9. Karthikeyan K., Kalpana D. and Renganathan N.G. (2009). Synthesis and characterization of ZnCo_2O_4 nanomaterial for symmetric supercapacitor applications. *Ionics*, 15, 107–110.
10. Trasatti S., Lipkowski J., Ross P.N. (1994). The Electrochemistry of Novel Materials. VCH Publishers, Weinheim, 207.
11. Omata K., Takada T. and Kasahara S. (1996). Active site of substituted cobalt spinel oxide for selective oxidation of COH_2 . Part II. *J. Appl. Catal. A: Gen.*, 146, 255-267.
12. Zhang G.Y., Guo B. and Chen J. (2006). MCo_2O_4 (M = Ni, Cu, Zn) nanotubes: Template synthesis and application in gas sensors. *Sens. Actuators B*, 114, 402-409.